AGU PUBLICATIONS

JGR

Journal of Geophysical Research: Atmospheres

RESEARCH ARTICLE
10.1002/2014JD021490

Key Points:
- Observed and model soil moisture-evaporative fraction relations largely agree
- Large inter-annual variability exists in the form of the relationship
- Evaporative fraction varies as a function of soil moisture and net radiation

Correspondence to:
T. W. Ford,
twford@tamu.edu

Citation:
Ford, T. W., C. O. Wulff, and S. M. Quiring (2014), Assessment of observed and model-derived soil moisture-evaporative fraction relationships over the United States Southern Great Plains, *J. Geophys. Res. Atmos.*, *119*, 6279–6291, doi:10.1002/2014JD021490.

Received 13 JAN 2014
Accepted 5 MAY 2014
Accepted article online 11 MAY 2014
Published online 3 JUNE 2014

Assessment of observed and model-derived soil moisture-evaporative fraction relationships over the United States Southern Great Plains

Trent W. Ford[1], Christoph O. Wulff[2], and Steven M. Quiring[1]

[1]Climate Science Laboratory, Department of Geography, Texas A&M University, College Station, Texas, USA, [2]GEOMAR Research Institute, Christian-Albrechts-Universität zu Kiel, Kiel, Germany

Abstract The relationship between soil moisture (SM) and evaporative fraction (EF) is an important component of land-atmosphere interactions. Frequently, land-atmosphere studies are based on land-surface models and not on observations. This study examines SM-EF interactions over the United States Southern Great Plains using both in situ observations and simulations from the Variable Infiltration Capacity hydrologic model. Specifically, we evaluate how the relationship between SM and EF varies by season, we determine why these variations occur, and we compare model-derived and observed SM-energy flux relationships. Data from four sites (2004–2008) that are part of the United States Department of Energy's Atmospheric Radiation Measurement—Southern Great Plains network are used in this study. Results show that SM-EF interactions in both the model and observations are in general agreement with the evaporative regime theory described in past studies. That is, EF is a linear function of SM when SM is between the wilting point and the critical value, and when SM is above the critical value, EF is not dependent on SM. However, SM-EF relationships vary substantially from year to year. EF is a linear function of SM only when daily net radiation is above normal. Our results suggest that the strength of SM-EF interactions is not solely controlled by soil wetness but is also strongly influenced by daily net radiation and meteorological conditions.

1. Introduction

Soil moisture can strongly modulate hydrologic and climatic conditions [*Pal and Eltahir*, 2001]. Dry soil can induce and amplify warm and dry conditions, especially during the summer by reducing local evaporation and modifying patterns of moisture convergence/divergence [*Taylor et al.,* 2012]. Therefore, soil moisture can have a strong impact on the surface Bowen ratio [*Quintanar et al.*, 2008], convective available potential energy [*Pal and Eltahir*, 2001], development of clouds [*Findell and Eltahir*, 2003], near-surface air temperature [*Mahmood et al.*, 2006], the likelihood of convective precipitation [*Frye and Mote*, 2010], planetary boundary layer depth [*Ek and Holtslag*, 2004], atmospheric circulation and the surface wind field [*Arrigo and Salvucci*, 2005; *Taylor et al.*, 2007; *Quintanar et al.*, 2009]. Soil moisture-atmosphere interactions in the North American Great Plains are strengthened by the high ratio of actual evapotranspiration to potential evapotranspiration [*Koster et al.*, 2009], and soil moisture provides a local moisture source.

Soil moisture-precipitation coupling in the North American Great Plains is difficult to quantify because much of the precipitation that occurs in the region is stratiform precipitation driven by remote moisture advection [*Frye and Mote,* 2010]. In addition, there is a lack of high quality, spatially extensive soil moisture observations [*Seneviratne et al.,* 2010]. The relationship between evapotranspiration and soil moisture is vital for understanding soil moisture-precipitation feedbacks [*Carleton et al.,* 2008; *Alfieri et al.,* 2008; *Jones and Brunsell*, 2009; *Myoung and Nielsen-Gammon*, 2010].

Previous studies have investigated the coupling between soil moisture and surface heat fluxes, both with land surface models and observations. *Dirmeyer et al.* [2000] used three land surface schemes to examine the relationship between the partitioning of latent and sensible heat and soil moisture (SM) at sites with different land cover. They demonstrated that surface energy partitioning was strongly controlled by SM in all three schemes, although the form of the relationship varied somewhat between schemes. *Basara and Crawford* [2002] used a correlation analysis to evaluate the relationship between observed SM and latent and sensible heat flux in central Oklahoma. They found strong, linear correlations between soil moisture and

Figure 1. United States Southern Great Plains study region and the location of the four sites from the Atmospheric Radiation Measurement-Southern Great Plains (ARM-SGP) network used in this study.

surface energy flux, representing strong land-atmosphere coupling on days that they identified as ideal (i.e., clear skies, low winds, and no recent precipitation). *Koster et al.* [2009] employed an atmospheric general circulation model to characterize hydroclimatological regimes around the globe. They used the relationship between temperature and precipitation as a proxy for SM-evaporation coupling and found that SM most strongly influences evaporation in semi-arid areas where decreases in precipitation were associated with increases in air temperature. *Brimelow et al.* [2011] proposed that reductions in latent heat flux due to dry soils resulted in a deeper, warmer boundary layer and less convective storms during the summer of 2002 in Alberta, Canada. These studies suggest that soil moisture can strongly influence the partitioning of latent and sensible heat flux, particularly under dry conditions when moisture is a limiting factor to evapotranspiration.

Because in situ observations of soil moisture and surface heat fluxes are not readily available, past efforts to study land-atmosphere interactions have predominantly relied on land surface models. This paper addresses this knowledge gap by evaluating surface-atmosphere relationships using both in situ observations and model-derived data. Here we examine the nature of the relationship between soil moisture and surface energy fluxes using data from four stations in the Southern Great Plains of the United States. Surface energy fluxes in this study are represented by evaporative fraction (EF), which is the ratio of latent heat (LE) to latent heat plus sensible heat (SH) (equation (1)). Therefore, EF represents the ratio of incoming energy used for evapotranspiration compared to the total amount of incoming energy. This study (1) evaluates how the relationship between soil moisture and surface energy partitioning varies by location and by season, (2) examines why these variations occur, and (3) compares the model-derived and observed soil moisture-energy flux relationships.

$$\mathrm{EF} = \frac{\mathrm{LE}}{\mathrm{LE} + \mathrm{SH}} \tag{1}$$

2. Data and Methods

2.1. Observations

Data from four sites in Kansas and Oklahoma that are part of the United States Department of Energy's Atmospheric Radiation Measurement—Southern Great Plains (ARM-SGP) network are used in this study (Figure 1). ARM-SGP measures numerous meteorological and hydrological variables, and these data

are available from: http://www.arm.gov/. We utilized 30 min measurements of volumetric soil water content (SM, cm^3/cm^3), latent heat flux (LE, W/m^2), and sensible heat flux (SH, W/m^2) as well as hourly measurements of downward shortwave radiation (W/m^2). The four sites in Kansas and Oklahoma were selected because they have relatively complete data between 2004 and 2008, and the sites span a diverse range of vegetation and soil types.

Soil volumetric water content at ARM-SGP sites is measured using the Soil Water and Temperature System (SWATS). SWATS uses a Campbell Model 229-L Matric Potential Sensor to provide matrix potential at 5, 15, 25, 35, 60, 85, 125, and 175 cm [*Bond*, 2005]. Soil water content is measured in two different locations at each site to facilitate quality control. The data are subjected to a rigorous quality control-quality assurance procedure as described by *Bond* [2005]. SWATS soil moisture observations are provided at 30 min temporal resolution. Soil moisture at 5 cm was used to represent the 0–10 cm layer, compatible with the land surface model. We averaged 5 cm soil moisture data between 7:30 a.m. and 4:30 p.m. (local time), coinciding with the daily averaging of model-simulated soil moisture, to arrive at a "day-time" average soil moisture observation.

LE and SH are derived using the Energy Balance Bowen Ratio (EBBR) method which uses observations of net radiation, soil surface heat flux, and the vertical gradients of temperature and relative humidity [*Cook*, 2011]. The EBBR sensors have an expected uncertainty of 10% for LE and SH, representing the range of probable maximum deviation of a measured value from the true value within a 95% confidence interval [*Cook*, 2011]. LE and SH estimates from eddy covariance systems are available at a few ARM sites. However, the eddy covariance systems are placed over cropland [*Cook*, 2011], while the SWATS soil moisture sensors are placed under grassland. Therefore, we use the EBBR system, which is placed over grassland, because of the land cover type match with the SWATS sensors. Similar to the SWATS soil moisture data, the EBBR flux data are subjected to a rigorous quality control-quality assurance procedure as described by *Cook* [2011]. The 30 min observations between 7:30 a.m. and 4:30 p.m. (local time) were averaged to provide "day-time" average LE and SH.

Daily net radiation data from the Oklahoma Mesonet site at El Reno (www.mesonet.org) is used to quantify the impact of net radiation on the SM-EF relationship. Oklahoma Mesonet data are used instead of the solar radiation data from the ARM network because of issues with missing data and data quality at the ARM site. The El Reno Oklahoma Mesonet site is approximately 3 km from the El Reno ARM site, and therefore it is assumed to represent radiation conditions for the ARM site. Daily net radiation (MJ/m^2) is measured with a Kipp & Zonen NR LITE net radiometer at 1.5 m.

2.2. Model

Land surface models provide a means for simulating soil moisture variability. However, model validation with in situ observations is important to constrain the simulated hydrological and meteorological processes and feedbacks. The model simulations generated in this study are compared with in situ observations at the ARM sites. We used the Variable Infiltration Capacity (VIC) model [*Liang et al.*, 1994], a macroscale hydrological model, to calculate the water and energy balances at the four ARM-SGP sites. VIC model version 4.1.2 [*Dan et al.,* 2012] was run for a period of 59 years (1950–2008), using 1950–2000 as the spin-up period. The model calibration data set detailed in *Sheffield et al.* [2006] was used to calibrate all model soil and vegetation parameters. Some information about the soil parameters at the ARM sites are available such as percent sand/silt/clay and bulk density. However, details regarding how these parameters were calculated were not available, and all of the soil parameters that are needed by VIC were not available. Therefore, the soil parameters in *Sheffield et al.* [2006] were used. The only change that was made was to specify the land cover so that it was consistent with the observed conditions. The land cover at each ARM-SGP sites was determined by reviewing site photographs. Model vegetation parameter values over each grid cell were set to the default values in the *Sheffield et al.* [2006] data set.

The ARM-SGP network measures precipitation at daily and sub-daily resolution at some sites. However, these data were only available at two of the four sites used in this study. The meteorological data that were available contained many missing values and in many instances recorded precipitation events when nearby precipitation gauges did not. Therefore, the VIC model was forced with daily observations of precipitation, and minimum and maximum temperatures from the closest Global Historic Climatology Network (GHCN) station to each of the ARM-SGP sites. The distance between the GHCN station and ARM-SGP site was less

than 10 km in all cases. Wind speed is not measured at GHCN sites. Wind speed data were extracted from the global meteorological forcing data set developed by the Land Surface Hydrology Research Group at Princeton University [*Sheffield et al.*, 2006]. This data set is based on the National Centers for Environmental Protection—National Center for Atmospheric Research (NCEP-NCAR) 1° reanalysis product and has been bias corrected for elevation [*Sheffield et al.,* 2006].

VIC-simulated latent and sensible heat flux (W/m^2) and volumetric water content at 3 h output were averaged between 7:30 a.m. and 4:30 p.m. to capture day-time average conditions. VIC calculates soil moisture in three layers: 0–10 cm, 10–40 cm, and 40–100 cm. ARM soil moisture observations were averaged to better correspond with the modeled soil moisture. The 0–10 cm VIC soil moisture was compared to the 5 cm ARM measurement, the 10–40 cm VIC soil moisture was compared to the average of the 15, 25, and 35 cm ARM measurements, and the 40–100 cm VIC soil moisture was compared to the average of the 60 and 85 cm measurements. Net radiation (MJ/m^2) was also simulated by the VIC model to compare with observed radiation. The 3 h output from the VIC model was summed between 7:30 a.m. and 4:30 p.m. (local time) to estimate daily total net radiation.

2.3. Methods

We use the evaporative fraction (EF) which is the ratio of latent heat to total surface energy flux.

Volumetric water content is dependent on site-specific soil conditions and cannot be directly compared between study sites. Therefore, soil moisture was standardized by converting volumetric water content into percentiles. Daily soil moisture data at each site are used to generate an empirical distribution function. Separate distribution functions were derived for each site, and they are also derived separately for the model-simulated and observed soil moisture; a total of eight distribution functions (one model-based function and one observation-based function for each of the four sites). Daily volumetric water content values are subsequently converted to a percentile, representing the percent of daily volumetric water content values less than that particularly value. Therefore, the 100^{th} percentile, or a percentile value here of 1, represents the wettest soil conditions measured at a particular site over the entire study period, while the 0 percentile represents the driest soil conditions. Hereafter, SM is reported as percentiles of volumetric water content.

2.4. Experimental Design

Previous studies have determined that the nature of the SM-EF relationship is dependent on whether the situation is soil moisture limited or energy limited. *Dirmeyer et al.* [2000] demonstrated that SM-EF relationships in land surface models are characterized by two disparate regimes. When soil moisture is between the wilting point and critical value (typically 80% of field capacity), evaporation is strongly controlled by soil water content, and there is a linear relationship between SM and EF. When soil moisture is not limited (soil moisture $>$ critical value), evaporation is controlled by available energy. Under this regime, evaporation is essentially decoupled from soil moisture (i.e., uncorrelated with soil moisture). *Dirmeyer et al.* [2000] evaluated three different land surface models and found that these two modes of behavior were present in all of them. *Seneviratne et al.* [2010] also defined two evapotranspiration regimes, soil moisture limited and energy limited. SM-EF interactions in the soil moisture-limited regime are typically linear and strongest when soil moisture is between the wilting point and a critical value [*Seneviratne et al.*, 2010]. With this in mind, we evaluated the relationship between daily SM and EF at the four ARM sites. We then compared the observed SM-EF relationships with the VIC-simulated SM-EF relationships. A *t* test is used to assess the statistical significance of the slope of the linear relationship between SM and EF. This test evaluates whether the slope of the linear fit is significantly different from 0, and significance is again based on the 95% confidence interval.

3. Results

3.1. Relationship Between SM and EF

We examine the SM-EF relationship during the North American growing season (May–October, 184 days) between 2004 and 2008. Over the 20 growing seasons (four sites, 5 years) that we examined in this study, there is a great deal of variability in the observed SM-EF relationship and evidence of both linear and nonlinear interactions. The relationship between SM-EF appears to be constrained by SM, as EF responds most strongly to changes in SM when SM is below the 30^{th} percentile (Figure 2a). However, when SM is

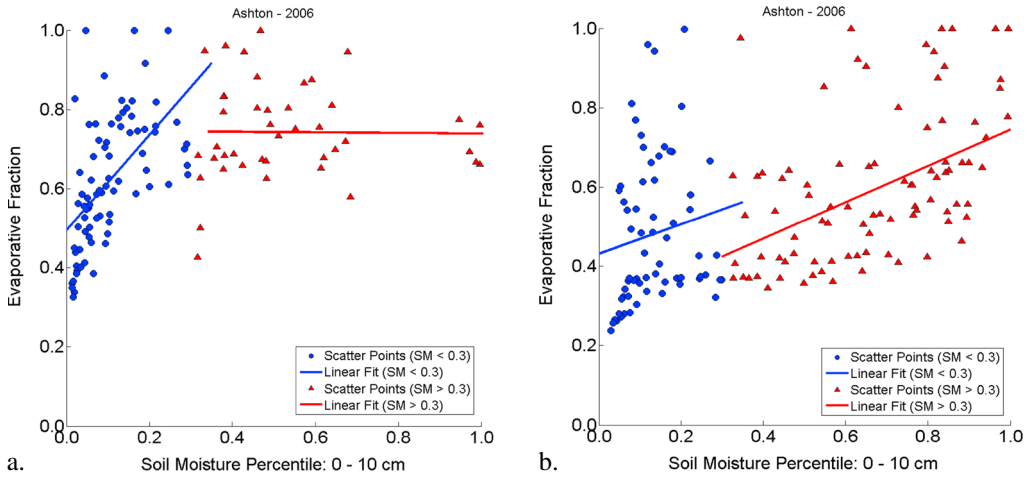

Figure 2. Soil moisture percentiles (0 to 10 cm) versus evaporative fraction in Ashton, Kansas based on (a) in situ observations and (b) VIC simulations. Each point represents a daily average; all days during the 2006 growing season are shown. The blue (red) line is the best fit line between SM and EF when SM is $<30^{th}$ ($>30^{th}$) percentile. Each graph contains 184 days (data points).

greater than the 30th percentile, there is little to no relationship between SM and EF. This pattern reflects, to some extent, the nonlinear relationships between SM and EF that are reported in *Dirmeyer et al.* [2000] and *Santanello et al.* [2007]. Figure 2 shows the observed relationship between SM and EF in Ashton, Kansas during the 2006 growing season. The best fit lines for the SM-EF relationships are based on 184 daily data points. The critical value used in *Dirmeyer et al.* [2000] represented 80% of field capacity; however, it is not possible to directly convert this value into a volumetric water content percentile. Because we use soil moisture percentiles, we are not able to use a physically based critical value like *Dirmeyer et al.* [2000]. Therefore, the critical value we use here is the 30th percentile, based on the observed change in the SM-EF relationship when soils are drier (less than) or wetter (greater than) the 30th percentile. The plots are divided into two parts using the 30th percentile of SM as the critical value. The relationship between SM-EF based on the in situ observations is statistically significant when SM is less than the 30th percentile, compared to an insignificant relationship when SM is greater than the 30th percentile. The model-simulated SM-EF relationship differs from that based on the in situ observations. The model-simulated relationship between SM-EF is only weakly linear when SM is less than the 30th percentile and the slope of the best-fit line does not change much when SM is greater than the 30th percentile. In fact, the model SM-EF relationship is statistically significant for both soil moisture conditions. The SM-EF relationship based on the observations reflects the dual regime behavior, where EF is a strong function of SM when SM is below the critical value; however, the model-simulated SM-EF does not show the same response. To determine how often SM-EF interactions display the dual regime behavior in both the observations and model, we calculate the slope of a least squares line when SM is less than the 30th percentile, and we calculate the slope of a least squares line when SM is greater than the 30th percentile. Each station and each growing season are treated separately. Tables 1 and 2 display the mean slope of the least squares line and the range of slope values at each station over all five growing seasons; Table 1 provides results for the observed SM and EF, and Table 2 provides results from the model-derived SM and EF.

Table 1. Summary of the Slope of the Best Fit Lines for SM-EF at Each Station Based on the In Situ ARM Observations[a]

Station	Soil Moisture	Slope Range	Mean Slope
Ashton	SM < 0.3	0.18–1.21	0.69
	SM > 0.3	−0.08–0.00	−0.03
Coldwater	SM < 0.3	−0.55–1.47	0.67
	SM > 0.3	0.08–0.40	0.18
Cordell	SM < 0.3	0.28–1.87	0.91
	SM > 0.3	−0.05–0.11	0.07
El Reno	SM < 0.3	−0.14–1.54	0.70
	SM > 0.3	−0.19–0.08	−0.02

[a]A least squares line is fit to each growing season (2004–2008), and the mean slope and the range of the slope parameters are reported. Two slopes are calculated for each growing season, one is based on all days when SM is <0.3, and one is based on all days when SM is >0.3.

When SM is less than the 30th percentile, there is a stronger linear relationship

Table 2. Summary of the Slope of the Best Fit Line for SM-EF at Each Station Based on the VIC-derived SM and EF[a]

Station	Soil Moisture	Slope Range	Mean Slope
Ashton	SM < 0.3	0.27–1.16	0.63
	SM > 0.3	0.02–0.48	0.21
Coldwater	SM < 0.3	0.51–1.86	1.24
	SM > 0.3	0.31–0.42	0.38
Cordell	SM < 0.3	0.22–1.04	0.74
	SM > 0.3	0.35–0.51	0.42
El Reno	SM < 0.3	0.58–1.71	0.44
	SM > 0.3	0.16–0.50	0.36

[a]A least squares line is fit to each growing season (2004–2008), and the mean slope and range for the slope parameters are reported. Two slopes are calculated for each growing season, one is based on all days when SM is <0.3, and one is based on all days when SM is >0.3.

between SM-EF (larger slopes), based on the observations, than when SM is greater than the 30th percentile. A test of the significance of the slope of the linear SM-EF fit when SM is less than the 30th percentile shows that the slope is significantly different from 0 (positive or negative) in 18 out of 20 growing seasons. At the same time, the slope of the lines based on days when SM is greater than the 30th percentile during those 18 growing seasons is not significantly different from 0. This suggests that the observed relationship between SM and EF frequently exhibits the dual regime behavior identified in previous studies. Similarly, the model-derived SM-EF relationships (Table 2) also show that when SM is less than the 30th percentile, the slope is significantly different from 0 in 15 out of 20 growing seasons, while the slope when SM is greater than the 30th percentile during those 15 growing

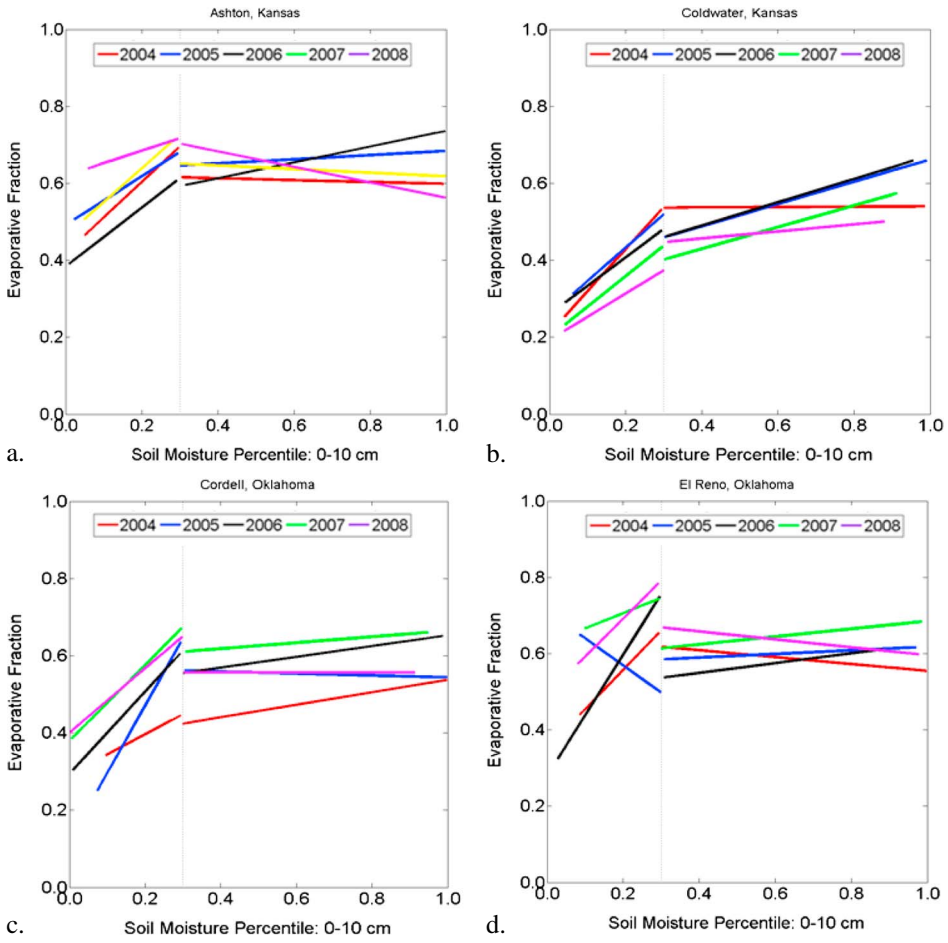

Figure 3. Observed soil moisture (0–10 cm) and evaporative fraction from ARM in situ measurements. The lines represent the linear fit between daily soil moisture and evaporative fraction. The relationship fit is assessed separately for days when soil moisture is less than the 30th percentile, and days when soil moisture is greater than the 30th percentile, separated by the vertical black line. Fit lines are color coded by year. Each year contains 184 days, from which the two regimes are fitted.

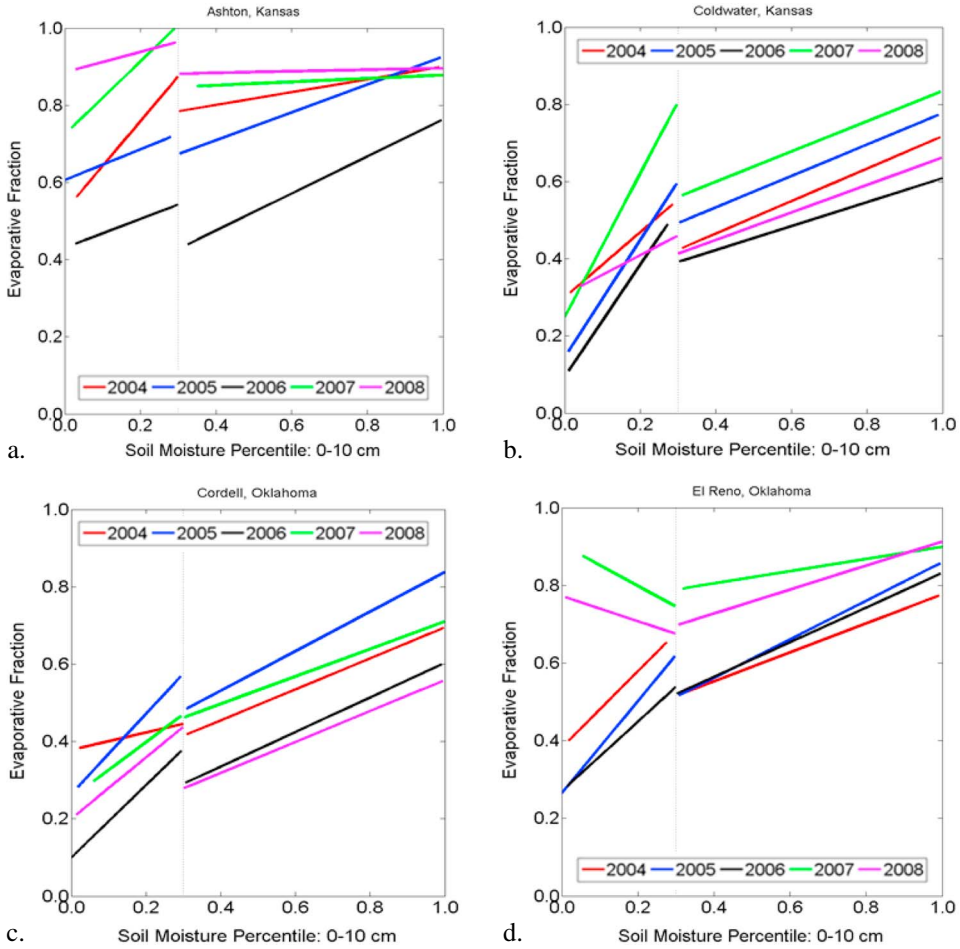

Figure 4. Model-derived soil moisture (0–10 cm) and evaporative fraction from the Variable Infiltration Capacity model. The lines represent the linear fit between daily soil moisture and evaporative fraction. The relationship fit is assessed separately for days when soil moisture is less than the 30th percentile, and days when soil moisture is greater than the 30th percentile, separated by the black, dotted line. Fit lines are color coded by year. Each year contains 184 days, from which the two regimes are fitted.

seasons is not significantly different from 0. Therefore, EF is often strongly modified by SM, in both the observations and model, when SM is less than the critical value (i.e., SM is limited).

There is noticeable interannual variability in the relationship between SM-EF. To better document this variability, we plot the linear relationship between observed SM-EF for all four stations, separating the data by year (Figure 3). Each line in Figure 3 shows the linear fit between daily SM and EF, and fits are assessed separately for days when soil moisture is less than and greater than the 30th percentile (our critical value). Each year of the study period includes 184 days, from which the fit is assessed in the two regimes. There is substantial year-to-year variability in the slope of the linear fit, especially at Cordell and El Reno. Figure 4 shows the same information as Figure 3, except the linear fits are shown for model-derived SM-EF data. The model-derived SM-EF relationships at Cordell and Coldwater are less variable than the model-derived SM-EF relationships at Ashton and El Reno. In general, the SM-EF relationships in both the observed and model-simulated data sets are similar to those reported in previous studies [e.g., *Santanello et al.,* 2007]. During most years, EF responds most strongly (linearly) to soil moisture variations below the 30th percentile.

Interestingly, the SM-EF fit for El Reno in 2007 and 2008 is very different than the other 3 years at El Reno. The majority of years exhibit the dual regime behavior of EF with respect to SM. However, the SM-EF relationships in El Reno during 2007 and 2008 do not exhibit this behavior. The reasons for this interannual variability in the nature of the SM-EF relationship are examined in the following section.

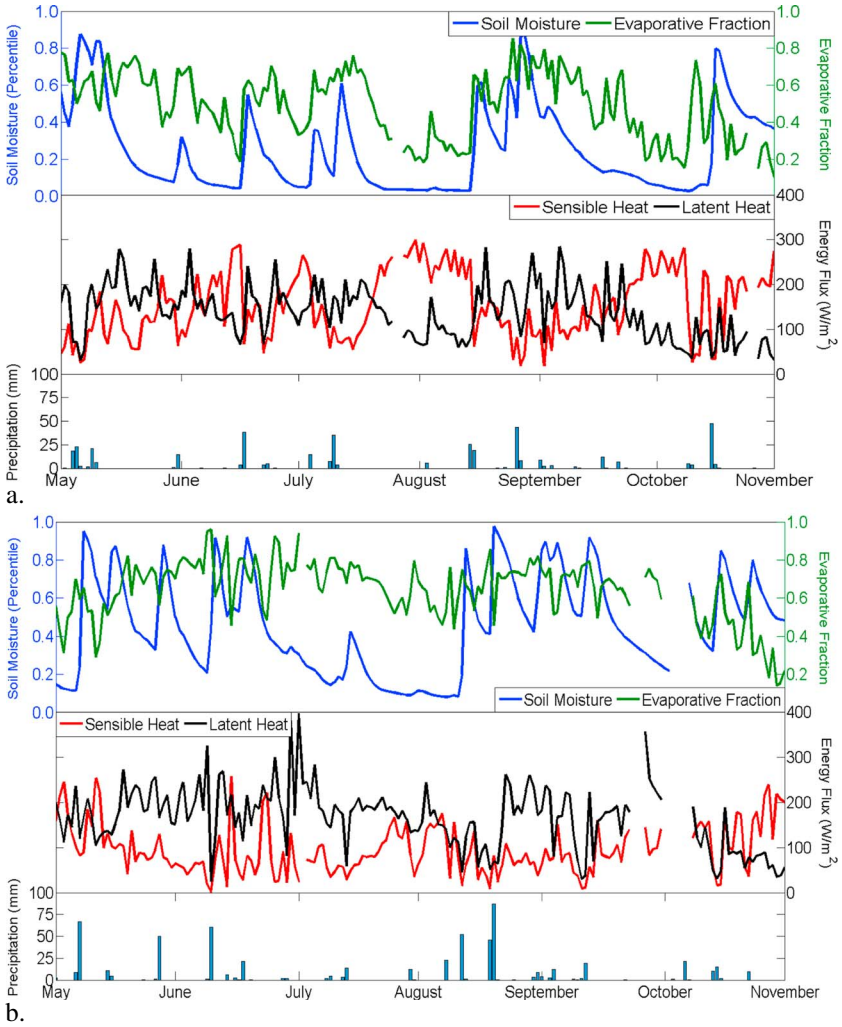

Figure 5. Soil moisture and meteorological conditions at El Reno, Oklahoma from May through October in (a) 2006 and (b) 2008. For each figure, the top panels show daily, 0–10 cm soil moisture percentiles (blue) and evaporative fraction (green), the middle panels show sensible heat (W/m^2) (red) and latent heat (W/m^2) (black), and the bottom panels show daily precipitation (mm).

3.2. Variability in the Observed SM-EF Relationship

SM-EF interactions during the majority of growing seasons are represented by the dual regime behavior described in the previous section. The 2006 growing season at El Reno is a good example of how the observed SM-EF relationship agrees with the dual regime behavior (Figure 5a). SM rapidly increases following a precipitation event (Figure 5a), and this is followed by an increase in EF. Several consecutive days with little or no precipitation correspond with slow, consistent drying of the soil and decreases in EF. EF is most strongly influenced by SM when it is below the 30th percentile. Both the observed (Figure 3d) and model-simulated (Figure 4d) SM-EF relationships show this dual regime behavior during 2006 at El Reno. In contrast, EF varies nearly independently of SM in 2008 (Figure 5b), despite SM varying from very wet (95th percentile) to very dry conditions (5th percentile) during the growing season. Figure 5b shows a slow, consistent decrease in SM between mid-June and mid-August in 2008, while EF stays fairly constant. Meteorological conditions during these two growing seasons must account for the differences in the SM-EF interactions between 2006 and 2008 because other factors, such as soil texture and vegetation (land cover) type at the site, do not vary from year to year.

Figure 6 shows the distribution of SM during the 2006 (red) and 2008 (blue) growing seasons. Dry soils occurred much more frequently in 2006 than in 2008. In fact, SM was drier than the 30th percentile

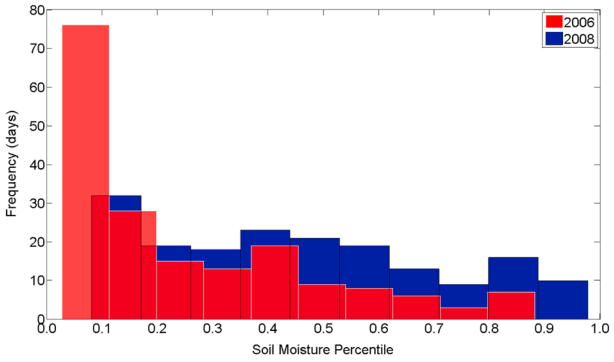

Figure 6. Histograms of soil moisture (percentiles) from May through October in 2006 (red) and 2008 (blue). The *y* axis represents number of days in each bin days. The bins of the two histograms are slightly offset for better visual comparison.

during 66% of days in 2006 compared with just 30% of days in 2008. The average number of consecutive days when SM was below the 30th percentile was 16 in 2006, compared with an average of 5 days in 2008. These differences in SM are due to marked differences in precipitation patterns in 2006 and 2008. In 2006, precipitation was nearly 125 mm less than the average (1895–2013) between May and October. Precipitation was nearly 45 mm above normal in 2008. Despite a prolonged period without rain during the 2008 growing season, the EF remained above 0.5 due to an abundance of precipitation during the early part of the growing season. There was a stronger relationship between SM and EF in 2006 because precipitation was well below normal and SM was the primary limiting factor for evapotranspiration.

3.3. Role of Net Radiation in SM-EF Interactions

A central element of the dual regime theory proposed in previous studies is that EF varies as a strong, linear function of SM when SM is below a critical value. SM-EF interactions in both the model and observations exhibit this behavior during many growing seasons (Figures 3 and 4); however, interannual variations in growing-season SM are insufficient to account for the large differences in the SM-EF interactions at El Reno between 2006 (precipitation was 125 mm below normal) and 2008 (precipitation was 45 mm above normal). Under the dual regime theory, EF should respond to soil drying, particularly when SM is below the critical value for a prolonged period of time. To better detail differences between SM and EF at El Reno in 2006 and 2008, we compare EF, SH, and SM during the 2006 and 2008 growing seasons (Figure 7). SM decreases between the middle of June and beginning of August in both years. In 2008, the decrease in SM does not correspond with a noticeable decrease in EF. In 2006, EF does not begin to noticeably decrease in response to the drying of the soil until sensible heat plateaus at over 200 W/m^2 until from late July to mid-August. A similar situation occurs in mid-September of that year, when EF decreases in response to both decreasing SM and increasing SH. In contrast, in 2008 EF does not respond to changes in SM despite prolonged periods when SM is below the critical value (30th percentile), although this time period in 2008 also corresponds with much lower SH values than the same time in 2006. This suggests that differences in the SM-EF relationships between 2008 and 2006 may be more strongly controlled by net radiation than SM.

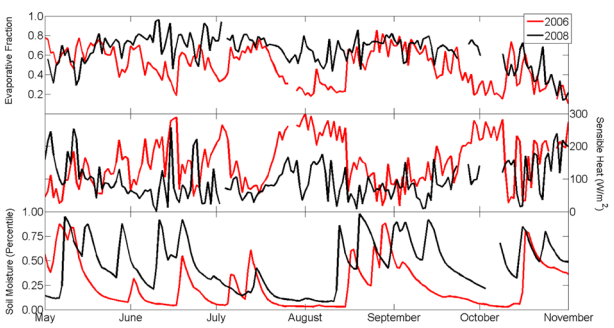

Figure 7. Plot shows (top panel) evaporative fraction, (middle panel) sensible heat, and (bottom panel) 0–10 cm soil moisture in El Reno, Oklahoma during the 2006 (red) and 2008 (black) growing seasons.

The impact of net radiation on SM-EF interactions was quantified by showing how the relationship between SM-EF changes as a function of daily net radiation at the surface. Figure 8 shows five plots of SM-EF interactions at El Reno that were created by sorting the data according to the quantile of daily net radiation (Q*) received at the surface (80th, 60th, 40th, and 20th percentiles). When we separate the SM-EF scatter points by Q* quantile, this creates a different number of data points for each quantile class. However, the number of data points in each quantile class is not highly variable, as the minimum

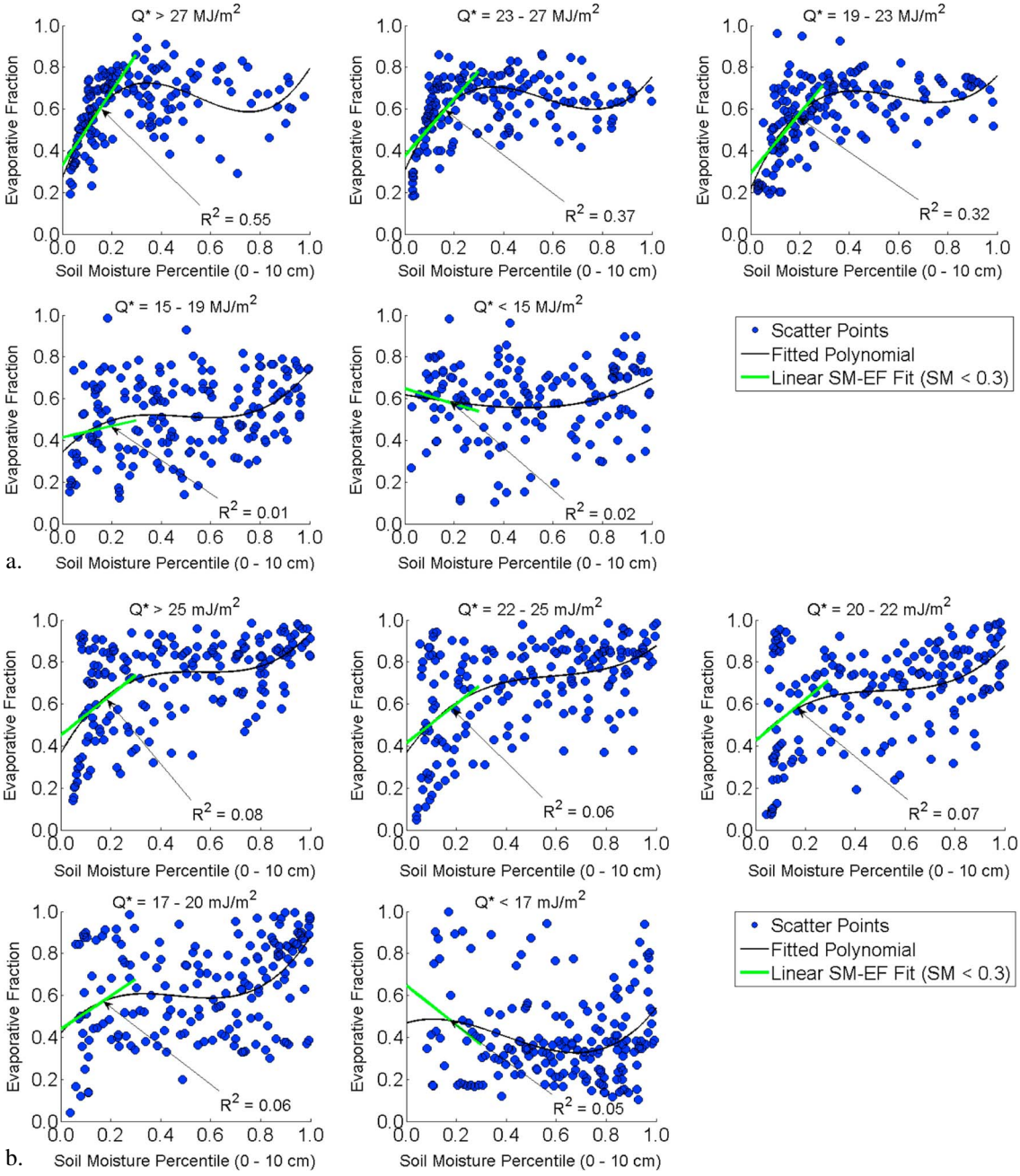

Figure 8. Soil moisture and evaporative fraction from (a) observations and (b) VIC model at El Reno, Oklahoma from 2004 to 2008 growing seasons. Daily data are separated based on the daily net radiation (Q*) received at the surface, and each plot shows SM-EF interactions under different net radiation percentiles. The black line represents the polynomial fit based on all days, and the green line shows the linear fit between SM and EF for days when the SM percentile is less than 0.3 (critical value). The R^2 values reported in the bottom right of each plot are based on the linear fit between SM and EF (green line).

number of points used to measure the SM-EF relationship in the observations (Figure 8a) is 68 (20^{th} Q* quantile) and the maximum number of points is 110 (80^{th} Q* quantile). The same is true for the model SM-EF scatter points (Figure 8b) as the number of points ranges from 65 (20^{th} Q* quantile) to 113 (80^{th} Q* quantile). The observed SM-EF data (Figure 8a) show that EF is a strong function of SM when SM is less than the 30^{th} percentile and net radiation is higher than normal (above the median). Specifically, SM explains 55% of the variance in EF when net radiation is greater than 27 MJ/m^2 and SM is less than the 30^{th} percentile. However, SM explains only 1% of the variance in EF when net radiation is less than 19 MJ/m^2 and SM is less than the

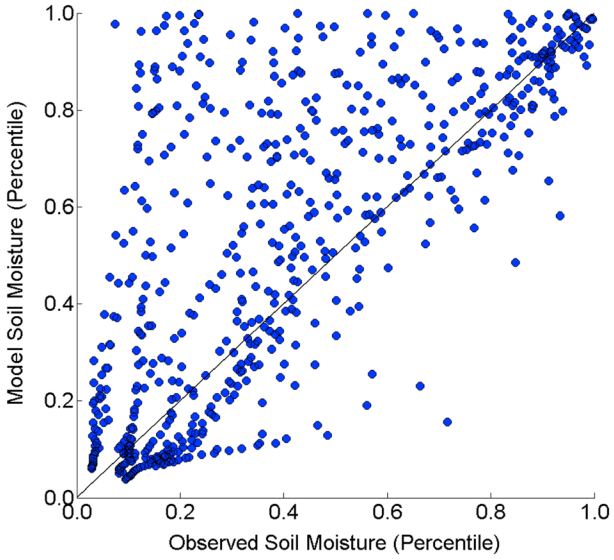

Figure 9. Observed 0–10 cm soil moisture (*x* axis) versus model-derived 0–10 cm soil moisture (*y* axis) at El Reno between 2004 and 2008. Each point represents a daily mean soil moisture value, and the black line represents the 1-1 fit.

30th percentile. The difference in the strength of the relationship between EF and SM is controlled by net radiation. Based on the observations, EF is essentially decoupled from SM on days when net radiation is below normal (e.g., cloudy days). On these days, SM is not strongly related to EF regardless of whether SM is above or below the critical value. This means that locations, such as the U.S. Great Plains, that are typically viewed as having a moisture-limited regime can also behave like an energy-limited regime [*Koster et al.,* 2009]. Therefore, the intra- and inter-growing-season variations in the strength and nature of the SM-EF coupling are, in part, determined by the meteorological conditions (e.g., cloud cover, net radiation).

Separating SM-EF interactions for the model-derived data by daily net radiation produces similar results, although much less of the variance in EF can be explained by SM. For example, SM explains only 8% of the variance in EF when daily net radiation is greater than the 80th percentile. The majority of SM-EF relationship interannual variability in the observations is attributable to differences in net radiation received at the surface (Figure 8a). However, differences in net radiation failed to explain the interannual SM-EF variability seen in the model (Figure 8b). The differences between the observed and model-simulated SM-EF relationship may be partially attributable to differences in SM immediately after a precipitation event. Figure 9 compares observed and modeled SM at El Reno (2004–2008). The model commonly simulates saturated conditions following a precipitation event (e.g., values near 1), while during these same days the observed SM is often much less.

4. Discussion

Dirmeyer et al. [2000] computed SM and EF on a global scale using three different land surface schemes. They separated all grid cells by vegetation type and determined the relationship between July SM and EF by fitting an arctangent function. They found that this function approximates the dual regime theory. The lines that we fit to the observed and model-simulated SM-EF (Figures 3 and 4) are similar to those presented in *Dirmeyer et al.* [2000]. Caution must be taken when directly comparing our results to those from *Dirmeyer et al.* [2000] because of the different "critical values" used between studies. That being said, based on the SM-EF slope analysis, 18 out of 20 growing seasons based on the observations and 15 out of 20 growing seasons based on the model agree with the dual regime theory. That is, during these growing seasons, EF is generally a linear function of SM when SM is below a critical value. In both the observations and model, the critical value for SM corresponds approximately with the 30th percentile. When SM is wetter than this, EF tends to function independently of SM conditions [*Seneviratne et al.,* 2010]. Our results confirm this finding and show that it is robust in both the observed and model-simulated SM-EF data at four sites in the U.S. Great Plains.

Despite confirming the dual regime behavior, we also found that there is considerable interannual variability in the observed and model-simulated SM-EF relationships. For example, the SM-EF relationship in 2007 and 2008 in El Reno does not fit the dual regime form. A more detailed analysis showed that net radiation has a strong influence on the SM-EF relationship. In the observations, EF varies as a function of SM when SM is less than the critical value and net radiation is above normal. *Basara and Crawford* [2002] found a similar relationship between SM and LH during the growing season in Oklahoma. Their results showed that LH varied as a strong, linear function of SM during "ideal days," characterized by clear skies, low near-surface wind

speed, and negligible precipitation during preceding days. In accordance with our findings, EF variability is not only constrained by soil water but also by net radiation and general atmospheric conditions (cloudiness, presence/absence of precipitation).

The ability of SM to impact near-surface atmospheric conditions depends on SM being the primary driver for partitioning latent and sensible heat [*Wei and Dirmeyer*, 2012]. *Koster et al.* [2009] suggest that SM can impact near-surface temperatures more strongly in the south-central U.S. than in other regions because of the tight coupling between SM and EF and sufficient intra-annual SM variability. *Koster et al.* [2009] demonstrated that because the Great Plains is a semi-arid region, it is typically characterized by a moisture-limited evaporative regime, which occasionally becomes energy limited. The differences in SM-EF interactions between 2006 (moisture limited) and 2008 (energy limited) in our results corroborate those of *Koster et al.* [2009]. In addition, our results suggest that the SM-EF relationship cannot be determined solely based on SM conditions. SM-EF interactions are a function of both SM and net radiation, and both of these variables are necessary to characterize land-atmosphere interactions, particularly in semi-arid environments such as the U.S. Great Plains. The impact that soil moisture has on atmospheric temperature, humidity, and subsequent precipitation is dependent on the strength of the relationship between soil moisture and evaporative fraction [*Findell et al.*, 2011]. Therefore, the results of this study are relevant for land-atmosphere interactions in general, as soil moisture is shown here to be strongly, linearly related to evaporative fraction under certain conditions, and these conditions are dependent on both soil moisture and the amount of available energy (net radiation).

5. Conclusion

Daily observations from four ARM sites and simulations from the VIC model are used to characterize SM-EF relationships. Overall, this study found that SM-EF interactions generally fit the dual regime behavior discussed in previous studies, but that the SM-EF relationship varies substantially from year to year. Our results suggest that although the U.S. Great Plains is typically identified as having a moisture-limited regime, both energy and moisture availability are important. The intra- and inter-growing-season variations in the strength and nature of the SM-EF coupling are, in part, determined by whether the moisture or energy conditions are the dominant control. Theory suggests that variations in EF are controlled by SM when SM is below the critical value; however, our results highlight the importance of both SM and energy (net radiation) across the entire spectrum of SM conditions. Specifically, SM influences EF most strongly when SM is less than the critical value and net radiation is ample; however, when net radiation is low, EF functions independently of SM, regardless of SM magnitude.

Acknowledgments
This research was funded by the National Science Foundation (award AGS-1056796). O.W. was funded by DAAD Research Internships in Science and Engineering. Data were obtained from the Atmospheric Radiation Measurement Program sponsored by the U.S. Department of Energy, Office of Science, Office of Biological and Environmental Research, Environmental Sciences Division.

References

Alfieri, L., P. Claps, P. D'Odorico, F. Laio, and T. M. Over (2008), An analysis of the soil moisture feedback on the convective and stratiform precipitation, *J. Hydrometerol.*, *9*(2), 280–291.

Arrigo, J., and G. Salvucci (2005), Investigation hydrologic scaling: Observed effects of heterogeneity and nonlocal processes across hillslope, watershed, and regional scales, *Water Resour. Res.*, *41*, W11417, doi:10.1029/2005WR004032.

Basara, J. B., and K. C. Crawford (2002), Linear relationships between root-zone soil moisture and atmospheric processes in the planetary boundary layer, *J. Geophys. Res.*, *107*(D15), 4274, doi:10.1029/2001JD000633.

Bond, D. (2005), *Soil Water and Temperature System (SWATS) handbook*, Atmospheric Radiation Measurement Climate Research Facility, U.S. Department of Energy, Washington D. C.

Brimelow, J. C., J. M. Hanesiak, and W. R. Burrows (2011), Impacts of land-atmosphere feedbacks on deep, moisture convection on the Canadian Prairies, *Earth Interact.*, *15*(31), 1–29, doi:10.1175/2011EI407.1.

Carleton, A. M., D. L. Arnold, D. J. Travis, S. Curran, and J. O. Adegoke (2008), Synoptic circulation and land surface influences on convection in the Midwest U.S. "Corn Belt" during the summers of 1999 and 2000. Part I: Composite synoptic environments, *J. Clim.*, *21*(14), 3389–3415.

Cook, D. R. (2011), *Energy Balance Bowen Ratio (EBBR) handbook*, Atmospheric Radiation Measurement Climate Research Facility, U.S. Department of Energy, Washington D. C.

Dan, L., J. Ji, Z. Xie, F. Chen, G. Wen, and J. E. Richey (2012), Hydrological projections of climate change scenarios over the 3H region of China: A VIC model assessment, *J. Geophys. Res.*, *117*, D11102, doi:10.1029/2011JD017131.

Dirmeyer, P. A., F. J. Zeng, A. Ducharne, J. C. Morrill, and R. D. Koster (2000), The sensitivity of surface fluxes to soil water content in three land surface schemes, *J. Hydrometeorol.*, *1*(2), 121–134.

Ek, M. B., and A. A. M. Holtslag (2004), Influence of soil moisture on boundary layer cloud development, *J. Hydrometeorol.*, *5*(1), 1525–7541.

Findell, K. L., and E. A. B. Eltahir (2003), Atmospheric controls on soil moisture-boundary layer interactions. Part I: Framework development, *J. Hydrometeorol.*, *4*(3), 552–569.

Findell, K. L., P. Gentine, B. R. Lintner, and C. Kerr (2011), Probability of afternoon precipitation in eastern United States and Mexico enhanced by high evaporation, *Nature*, *4*, 434–439.

Frye, J. D., and T. L. Mote (2010), The synergistic relationship between soil moisture and low-level jet and its role on the prestorm environment in the Southern Great Plains, *J. Appl. Meteorol. Climatol.*, *49*(4), 775–791.

Jones, A. R., and N. A. Brunsell (2009), Energy balance partitioning and net radiation controls on soil moisture-precipitation feedbacks, *Earth Interact.*, *13*(2), 1–25, doi:10.1175/2009EI270.1.

Koster, R., S. Schubert, and M. Suarez (2009), Analyzing the concurrence of meteorological droughts and warm periods, with implications for the determination of evaporative regime, *J. Clim.*, *22*(12), 3331–3341.

Liang, X., D. P. Lettenmaier, E. F. Wood, and S. J. Burges (1994), A simple hydrologically based model of land surface water and energy fluxes for general circulation models, *J. Geophys. Res.*, *99*(D7), 14,415–14,428, doi:10.1029/94JD00483.

Mahmood, R., S. A. Foster, T. Keeling, K. G. Hubbard, C. Carlson, and R. Leeper (2006), Impacts of irrigation on 20th century temperature in the northern Great Plains, *Global Planet. Change*, *54*(1-2), 1–18.

Myoung, B., and J. W. Nielsen-Gammon (2010), The convective instability pathway to warm season drought in Texas. Part I: The role of convective inhibition and its modulation by soil moisture, *J. Clim.*, *23*(17), 4461–4473.

Pal, J. S., and E. A. B. Eltahir (2001), Pathways relating soil moisture conditions to future summer rainfall within a model of the land–atmosphere system, *J. Clim.*, *14*(6), 1227–1242.

Quintanar, A. I., R. Mahmood, J. Loughrin, and N. C. Lovanh (2008), A coupled MM5-NOAH land surface model-based assessment of sensitivity of planetary boundary layer variables to anomalous soil moisture conditions, *Phys. Geogr.*, *29*(1), 54–78.

Quintanar, A. I., R. Mahmood, M. V. Motley, J. Yan, J. Loughrin, and N. Lovanh (2009), Simulation of boundary layer trajectory dispersion sensitivity to soil moisture conditions: MM5 and Noah-based investigation, *Atmos. Environ.*, *43*(24), 3774–3785.

Santanello, J. A., Jr., M. A. Friedl, and M. B. Ek (2007), Convective planetary boundary layer interactions with the land surface at diurnal time scales: Diagnostics and feedbacks, *J. Hydrometeorol.*, *8*(5), 1082–1097.

Seneviratne, S. I., T. Corti, E. L. Davin, M. Hirschi, E. B. Jaeger, I. Lehner, B. Orlowsky, and A. J. Teuling (2010), Investigating soil moisture–climate interactions in a changing climate: A review, *Earth Sci. Rev.*, *99*(3), 125–161.

Sheffield, J., G. Goteti, and E. F. Wood (2006), Development of a 50-year high-resolution global dataset of meteorological forcings for land surface modeling, *J. Clim.*, *19*(13), 3088–3111.

Taylor, C. M., D. J. Parker, and P. P. Harris (2007), An observational case study of mesoscale atmospheric circulations induced by soil moisture, *Geophys. Res. Lett.*, *34*, L15801, doi:10.1029/2007GL030572.

Taylor, C. M., R. A. M. de Jeu, F. Guichard, P. P. Harris, and W. A. Dorigo (2012), Afternoon rain more likely over drier soils, *Nature*, *489*(7416), 423–426.

Wei, J., and P. A. Dirmeyer (2012), Dissecting soil moisture-precipitation coupling, *Geophys. Res. Lett.*, *39*, L19711, doi:10.1029/2012GL053038.